Hindawi
Mobile Information Systems
Volume 2022, Article ID 8794029, 11 pages
https://doi.org/10.1155/2022/8794029

Research Article

Application of Rhino Modeling Software in Product Fading Surface Modeling Design from the Perspective of Computer

Jiahui Zhang

Kyungil University Graduate School, Kyungil University, Gyeongsan 38428, Gyeongsan, Republic of Korea

Correspondence should be addressed to Jiahui Zhang; 18409452@masu.edu.cn

Received 23 May 2022; Revised 2 July 2022; Accepted 13 July 2022; Published 30 August 2022

Academic Editor: Imran Shafique Ansari

In order to improve the effectiveness of product fading surface modeling design, this paper puts forward an application research of rhino modeling software in product fading surface modeling design from the perspective of computer. First, this paper studies the optimization design of product fading surface modeling, establishes the visual image information processing model of product fading surface modeling design, carries out product fading surface modeling design according to the information fusion results, and puts forward the product fading surface modeling design method based on visual expression and surface fusion. Based on rhino modeling software, the visual communication design of product fading surface modeling design is carried out, the visual optimization control model of product fading surface modeling is established, and the optimization design of product fading surface modeling is realized by combining the block fusion matching method. The simulation experiment of product fading surface modeling design is carried out in rhino modeling software. Therefore, this method has good effect, strong visual communication ability, and short time cost.

1. Introduction

Computer-aided geometric design (CAGD) is a new interdisciplinary subject. It was first proposed by Forrest in the UK in 1971. It mainly studies the representation, design, analysis, and specification processing of curves and surfaces. With the development of computer graphics, a new technology focuses more on curve and surface design, splicing, modeling, display, and morphological analysis [1]. As people have higher and higher requirements for product shape, product modeling has become more complex, and practical problems such as product design and manufacturing have a deeper connection with curve and surface modeling optimization. Modern young people have higher and higher requirements for product appearance, and product appearance design is no longer the pursuit of a single form, but more and more diversified. Good product appearance design not only conforms to people's aesthetic, plays a role in promoting product sales, but also can make the production of products more convenient, reduce consumption, reduce costs, and if the environmental adaptation and other factors are considered, can also play a role in environmental protection. So, what is the condition that the appearance design of the product must satisfy? Design form, as the name implies, is the shape of the product, which is also the most important requirement of the product in the appearance design. How can the designer combine the shape design with the internal structure, and also reflect some of the design innovation or other practical functions, is the top priority of the current product appearance design. Material selection: we all know that the material selection of product design is very key, and this determines the hardness and luster of the product in the appearance and also determines the product can be used in what kind of environment, so for the material selection of the product, we have to carry out the basic requirements, and it is necessary. Colors: in many cases, the consumer products interest is likely to be on the color appearance of the product is driven up, so the collocation of color to a great extent is to attract the customer's purchase desire, and because the visual sense is the direct feedback for the product first impression, the color collocation of this aspect is also the basic requirement of the product

appearance design. Feasibility: we want to know whether the appearance of the product design is feasible, because a lot of product appearance and its internal structure is tight, or have a very strong correlation, and is not the outward appearance is everything, so we need to analyze its feasibility; it has functions in many more representative of the products, and it is necessary.

In the process of solving these practical problems, new research ideas and methods continue to appear, and its application scope has become wider. Now, in addition to its application in the three major industries of aviation, automobile, and shipbuilding, it also extends to the fields of bioengineering, architectural design, D/m, electronic engineering, medical diagnosis, and clothing [2, 3]. Part of the reason why decorative materials are made depends on whether they are smooth, when in fact the material is curved and the surface is smooth enough. If not, this will ultimately lead to the aesthetics of the product. Therefore, it is important to study the human-machine surface optimization method suitable for the product [4].

At present, there have been many typical research results in the modeling design of fading surface of products. According to the modeling characteristics, the shape of complex products is simplified into a simple mesh model. Based on the principle of C-C surface mesh subdivision, a method of making product mesh model in product modeling design is proposed. After the user edits and modifies the mesh vertices for many times, the mesh subdivision is carried out, so as to obtain the customized modeling scheme of products. There is no need for a large number of surface editing operations, but there are some problems such as unclear surface modeling features and unsatisfactory matching accuracy [5]. In this paper, a forward and reverse hybrid design modeling method based on artecstudio, geomagicstudio, and CATIA software is proposed. The main purpose is to reduce the dimensional error between the modeling results and the actual object, but this method has the problem of large time cost. This paper summarizes the relevant research results of design-oriented free-form surface feature modeling technology and systematically studies the definition, classification, parameterization, editing, and extraction methods of free-form surface features. This method has a lot of theoretical support, but it has not been tested in practical application [6, 7]. Figure 1 shows the common practice of fading surface modeling. Rhino3D NURBS is a powerful 3d advanced modeling software. Its main function is 3D modeling, drawing 2d graphics, and dimensions. This software was introduced by RobertMcNeel in 1998. Compared with other 3D modeling software, this software requires less hardware equipment. All you need is an ISA graphics card and Windows 95. In addition, installing the software on a computer takes just over 20 megabytes. Although it is "a small sparrow", it is "five viscera". Rhino software is powerful and can be modeled very smoothly. It can create, analyze, and edit NURBS surfaces, curves, and entities with no restrictions on angle or size. It can quickly represent data into graphics, graphics design interface, 3-D graphics design character interface, working perspective window, unlimited graphics view area, designated view area, and toolbar interface.

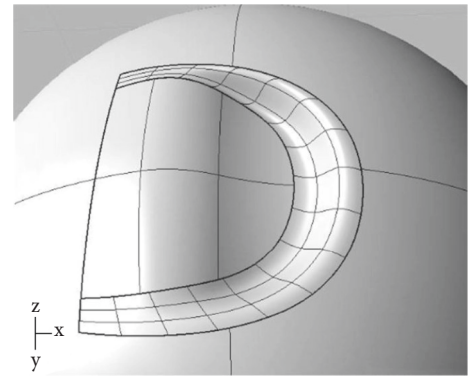

Figure 1: Common practice of fading surface modeling.

2. Literature Review

Burduhos nergis, D. P. and others proposed the spline mesh based on the optimization method, which is a method of "checking curves, surfaces, and modifications". The obvious disadvantage of this method is that the program needs to be checked and modified continuously in the process of the fairing, and its amount of calculation and modification is very large [8]. Messaoudene, A. and others proposed to use the Hermite element to minimize the target function and reproduce the C1 or C2 continuity of the surface in the whole field. This finite element interpolation calculation method combined with energy fairing makes the reconstructed surface not only have high precision but also have a good fairing. It is suggested to use the moving least square method to study curve and surface fitting [9]. Wang, H. and others proposed the research on curve and surface approximation algorithm based on cubic B-spline. The algorithm combines the respective advantages of interpolation spline and B-spline, avoids the shortcomings of traditional algorithms, and proves its convergence. The B-spline method cannot accurately describe the quadratic curve and the surfaces such as the sphere, while using the rational B-splines solves this problem. Tetteh, e. D. and others believe that in the modeling of product modeling design, a complete form consists of multiple single-sided splicing combinations, which can be expanded on the simple shape and add more details. This modeling form can be called face splicing [10]. Ali, F. and others set up a digital product modeling design course by using the modeling design software rhino, which can enable students to carry out three-dimensional modeling of product modeling design and understand the basic requirements of digital product modeling design, which will greatly improve students' homework level, graduation design level, and employment competitiveness [11]. Wang, X. and others believe that NURBS means nonuniform rational B-spline, which can be seen as freely making various forms of free curves according to the user's intention by using the control points and edit points existing between the

start point and the end point. NURBS can better control the curvature of the object surface than the traditional modeling method. Any imaginable shape can be obtained by using NURBS modeling [12]. Sunchenghao and others believe that in the modeling and design of three-dimensional surface modeling, the quality of the surface directly affects the appearance, comfort, and machining accuracy [13]. Jacobs, B. and others believe that the product modeling mouth is becoming more and more complex, and more and more curved surfaces are used. The design of curved surfaces should not only meet the aesthetic requirements of products but also better realize their functions, so as to meet the design performance requirements. The beauty of the surface depends on the smoothness, and the realization of the function depends on whether the product is easy to operate. Therefore, it is particularly important to find out the optimal design of the complex surface through certain methods [14]. Ali, F. and others believe that curve and surface fairing has an important impact on product design. Compared with most fairing optimization methods, the curve and surface energy method is a widely used method. It applies boundary constraints to deal with curves and surfaces and is suitable for large deformation and closed curve and surface fairing. However, it cannot guarantee the uniform change of curvature, and the least square method can make up for this deficiency [14]. Nakayama, M. and others used the improved energy method under physical constraints such as external load, established the energy model of curve and surface optimization according to the geometric constraints of the fairing, and studied the method of constructing the objective function of curve and surface under multidisciplinary theory [15].

3. Research Methods

3.1. Visual Communication Design and Image Processing of Product Fading Surface Modeling

3.1.1. Visual Communication Design. According to the similarity of different features, the local information measurement of the visual image of product fading surface modeling is carried out [12]. The block feature matching method is used for visual image processing and feature analysis of product fading surface modeling, and the visual segmentation model of product fading surface modeling is constructed. The generation sequence of visual features of product fading surface modeling is obtained as follows:

$$\mathrm{Dif}\left(C_1, C_2\right) = \min_{v_i \in C_1, v_j \in C_2, \left(v_i, v_j\right) \in \mathrm{E}} w\left(\left(v_i, v_j\right)\right). \tag{1}$$

In the above formula, $F_E = 1nI/1n\ D$ refers to the feature sampling point of the visual image of product fading surface modeling. The feature point of the visual image of product fading surface modeling is composed of the edge contour feature component of the image. Take k-nearest neighbors of the unknown sample, and reconstruct the visual image of product fading surface modeling according to the geometric distribution of the weak edge feature of the visual image of product fading surface modeling. The block structure model of visual communication of product fading surface modeling design is obtained, as shown in Figure 2.

According to Figure 2, the multilevel and multidirectional decomposition method is adopted to classify the image to be designed into the feature block subspace, and the local dynamic feature point detection output of the visual image of product fading surface modeling is obtained as follows:

$$I(x) = J(x)t(x) = A(1 - t(x)), \tag{2}$$

where A is the block pixel set representing the residual image and $t(x)$ is the detail separation eigenvalue of the visual image of product fading surface modeling.

3.1.2. Image Fusion and Filtering. Calculate the classified pixel set of product fading surface modeling visual image feature information, and obtain the estimated value of contour area distribution of product fading surface modeling visual image as follows:

$$\mathrm{NLM}[g](i) = \sum_{j \in \Omega} w(i, j) g(j). \tag{3}$$

Among them, the clustering center of visual reconstruction of product fading surface modeling is obtained by taking pixel I as the center. The image segmentation method is used to construct the visual feature sampling model of the image, when $0 \le w(i, j) \le 1$ and $\sum_{j \in \Omega} w(i, j) = 1$. It is assumed that the gray edge value of the visual image of product fading surface modeling obeys the Gaussian distribution; that is, $n \in N(0, \sigma_n^2)$, where σ_n^2 is the pixel intensity of visual imaging of product fading surface modeling. The detail separation method is used for block matching of all sample images, and the Euler–Lagrange equation is constructed according to the anisotropy of the image. The edge contour detection equation of the visual feature distribution of the product fading surface modeling is obtained as follows:

$$\begin{aligned}\frac{\partial \varphi}{\partial t} = {} & -\delta(\varphi)\left[\theta\left(\lambda_1 e_1^{\mathrm{LBF}} - \lambda_2 e_2^{\mathrm{LBH}}\right) + (1-\theta)\left(\lambda_1 e_1^{\mathrm{LGF}} - \lambda_2 e_2^{\mathrm{LGF}}\right)\right] \\ & + v\delta(\varphi)\mathrm{div}\left(\frac{\nabla\varphi}{|\nabla\varphi|}\right) + \mu\left(\nabla^2\varphi - \mathrm{div}\left(\frac{\nabla\varphi}{|\nabla\varphi|}\right)\right).\end{aligned} \tag{4}$$

e_1^{LBF}, e_1^{LBF}, e_2^{LBF}, e_1^{LGF}, and $e_2^{\mathrm{LGF}} e_1^{LGF}$, e_2^{LGF} are as follows:

$$\begin{cases} e_1^{\mathrm{LBF}} = \int_\Omega K_\sigma(y - x)\left|(x) - f_1(y)\right|^2 \mathrm{d}y \\ e_2^{LBF} = \int_\Omega K_\sigma(y - x)\left|(x) - f_2(y)\right|^2 \mathrm{d}y \end{cases}, \quad \begin{cases} e_1^{\mathrm{LGF}} = \int_\Omega K_\sigma(y - x)\left|I^G(x) - f_1^G(y)\right|^2 \mathrm{d}y \\ e_2^{\mathrm{LGF}} = \int_\Omega K_\sigma(y - x)\left|I^G(x) - f_2^G(y)\right|^2 \mathrm{d}y \end{cases}, \tag{5}$$

where $H(\varphi)$ is the block Heaviside function of the visual image of product fading surface modeling, and $\delta(z) = d/\mathrm{d}zH(z)$ is the Dirac function of edge contour

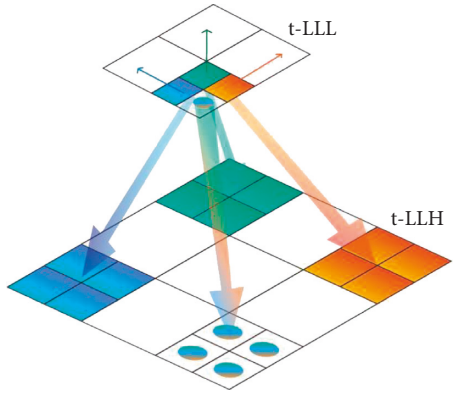

Figure 2: Block structure model of visual communication in product fading surface modeling design.

detection for product fading surface modeling design [16]. The local information is extracted from the low-frequency coefficient matrix, and the visual image fusion and filtering processing of product fading surface modeling are carried out in combination with the dynamic block segmentation technology.

3.2. Establishment of the Mathematical Model for Curve and Surface Optimization

3.2.1. Energy Method and Physical Constraints. In terms of mechanics, the physical spline is like an elastic thin beam with uniform properties under a concentrated load. Its optimization goal is to minimize the strain energy of a curved beam. The mathematical expression is

$$E = \beta \int_{\text{curve}} k^2 \mathrm{d}s. \tag{6}$$

In the above formula, β is the stiffness coefficient of the spline. This mathematical model comprehensively considers the two aspects of minimum energy and parameterization of expression. It has the characteristics of natural fairing. The physical energy model includes two parts of energy: bending resistance and tensile resistance, as shown in the following formula:

$$E = \int (\alpha E_s + \beta E_b) d\sigma, \tag{7}$$

where $\alpha\beta$ is the weight coefficient. The curves and surfaces generated by this model have no redundant wrinkles, which can also be said to be more smooth.

From the point of view of physical deformation energy, Terzopoulos and Gossard proposed the following model as formula (8) with the help of the thin plate elastic deformation equation in elasticity.

$$E_{\text{curve}} = \int \left(\alpha w_u^2 + \beta w_{uu}^2 - 2 f w\right) \mathrm{d}u, \tag{8}$$

where w is the calculated curve (surface) with u and v as parameters; $w_u, w_v, w_{uu}, w_{vv} w_{uv}$ are partial derivative vectors; $\alpha\beta$ is the given external load vector function.

For a clearer and intuitive explanation of $\alpha\beta$ and the physical meaning of F, the Euler equation is introduced here as equation (10):

$$\beta \frac{d^4 W}{\mathrm{d}u^4} - \alpha \frac{d^2 W}{\mathrm{d}u^2} = f. \tag{9}$$

It can be seen from (10) that it is similar to the elastic deformation equation, so $\alpha\beta$ is also a given material characteristic parameter, which mainly determines the ability of an object to resist deformation; F is the external load.

Since this paper mainly studies the optimization of B-spline curves and surfaces, we introduce the expression as follows:

$$W(u) = \sum_{i=0,m} V_i B_{i,s}(u). \tag{10}$$

The first and second derivative vectors of the curve obtained from (11) are equations (12) and (13), respectively.

$$W_u(u) = \sum_{i=0,m} V_i \dot{B}_{i,s}(u). \tag{11}$$

$$W_{uu}(u) = \sum_{i=0,m} V_i B''_{i,s}(u). \tag{12}$$

From the above formula, we can know that since the density s and node vector are known, formula (12) is transformed into integrating the known function. In order to obtain the unknown V (the control point of the curve), we only need to solve the above equation (quadratic function equation).

Now, most of the curve surface optimization is using some geometric constraints, such as using its type value point and control point and guide vector. In this section, the optimization of curves and surfaces is studied based on physical constraints, and the structural modeling of curves and surfaces is controlled by considering three physical attributes: external load, material properties, and boundary support. This method takes more consideration of the actual situation and has more application value [17, 18].

3.3. Curve and Surface Optimization Based on Improved Particle Swarm Optimization Algorithm

3.3.1. Basic Particle Swarm Optimization Algorithm. Particle swarm optimization algorithm (PSO), such as genetic algorithm and ant colony algorithm, is also a colony intelligence algorithm. Due to its fast speed and good robustness in multidimensional spatial function and dynamic target optimization, it has been widely used in the optimization and evolution fields of function optimization, fuzzy system control, and neural network training. With more and more research on it, we can roughly divide the research direction into four aspects: the algorithm itself, the parameter selection, the topology, and the integration with other evolutionary technologies. Among them, the combination with other algorithms is a hot topic

in the research of particle swarm optimization. There are usually two ideas of introducing genetic idea and ant colony idea. In addition, there are many hybrid PSO algorithms, such as gradient descent, immune algorithm, and K-means clustering algorithm. Because the particle swarm optimization algorithm does not need to set many parameters and the gradient information of the evolution process, it is very easy to implement. It plays an important role in solving nonlinear continuous optimization problems. Moreover, it also has very good controllability for those problems that cannot get satisfactory results optimized by common methods. Therefore, the particle swarm optimization algorithm has a wide range of applications [17].

The steps of the standard particle swarm optimization algorithm are as follows:

(1) Initialize particle swarm, initialize the velocity VI and position Xi of particles in the population, and set the population size M and the dimension n of particle solution space.

(2) Calculate the current fitness value of each particle according to the fitness function.

(3) Evaluate the fitness value of each particle in step (2), store the fitness value of each particle and its current position in the particle's respective pbest, compare the fitness value of each particle with the individual extreme value, if its fitness value is better, continue to update the individual extreme value, and save the updated satisfactory individual extreme value in the pbest. If the individual extreme value is better, keep it unchanged and store it in gbest.

(4) Compare all current in pbest and gbest to update gbest.

(5) If the termination conditions are met (usually the number of iterations or the actual required accuracy), stop the search and output the results. Otherwise, return to step.

3.3.2. Basic Steps of Genetic Algorithm Optimization. First is the population setting; since the basis of the genetic algorithm is population, setting the appropriate population size is of great significance to the operating performance of the genetic algorithm. If the population size is relatively large, it means that there are a variety of individuals in the population, so the algorithm may not fall into the situation of a local solution. However, if the population is too large, the amount of calculation will increase a lot, which increases the complexity of the calculation process. When the population size is too small, the search space of the genetic algorithm is limited, which may produce immature convergence results. The second is to initialize the population; because the initial individuals of the general population are randomly generated, it is difficult to judge the number and distribution of the optimal solution in the corresponding feasible solution space without knowing the initial empirical knowledge of the solution space of the target problem. Therefore, it is often used to randomly generate a certain number of individuals with uniform distribution in the solution space. And select good and qualified individuals from these individuals to form the initial species group. Third is the genetic parameter coding; the coding of parameters must be based on the actual situation of the target problem to be solved. It transforms the actual problem into computer binary code to form a solution space, and its genetic algorithm searches the optimal solution in this space [14, 16].

It has the following characteristics: (1) The processing object of the genetic algorithm is the encoded individual, not the parameter itself. (2) It can deal with multiple individuals in the population at the same time, rather than the traditional search for one individual, which solves the risk of falling into the local optimal solution. (3) The constraints of genetic algorithm are not affected by discontinuity and nondifferentiability. It uses the fitness function to evaluate individuals. (5) It has the characteristics of autonomous learning, adaptation, and self-organization. The basic steps of genetic algorithm operation are shown in Figure 3.

Comparison between genetic algorithm and ant colony algorithm: ant colony algorithm, which belongs to intelligent optimization algorithm, has certain memory. Ant colony algorithm has several principles, such as foraging principle and obstacle avoidance principle. It issues instructions based on pheromones in the environment. The genetic algorithm belongs to a group of intelligent optimization algorithms with parallelism. Each particle can actively choose to impersonate. The genetic algorithm is based on the biological evolution idea of survival of the fittest. The genetic algorithm has three kinds of operators: selection, crossover, and mutation. Each operator has its own different methods. Different improvement results can be obtained by modifying the operators and configuration methods.

3.3.3. Basic Ant Colony Algorithm. The essence of the ant colony optimization algorithm is the process that ants transmit information through pheromones, cooperate with each other, and finally find the shortest distance from the ant nest to the food source, that is, the optimal solution of the problem. If there are a large number of ants passing along a certain route, the greater the probability that it will be selected by later ants. It is composed of three mechanisms: route probability selection mechanism (the more pheromones secreted by ants on a route, the greater the probability that the route will be selected by later ants), pheromone update mechanism (the faster the amount of pheromones will increase on the shorter route), and collaborative work mechanism (pheromones deliver messages). It has the following characteristics: (1) distributed control, and each individual can only directly perceive the information of the local area; (2) the search process starts from multiple points at the same time, which greatly improves the optimization efficiency and response ability of the whole algorithm process; (3) it has autonomy and cooperation, and the optimization process does not depend on the mathematical properties of the optimized problem itself; (4) probabilistic

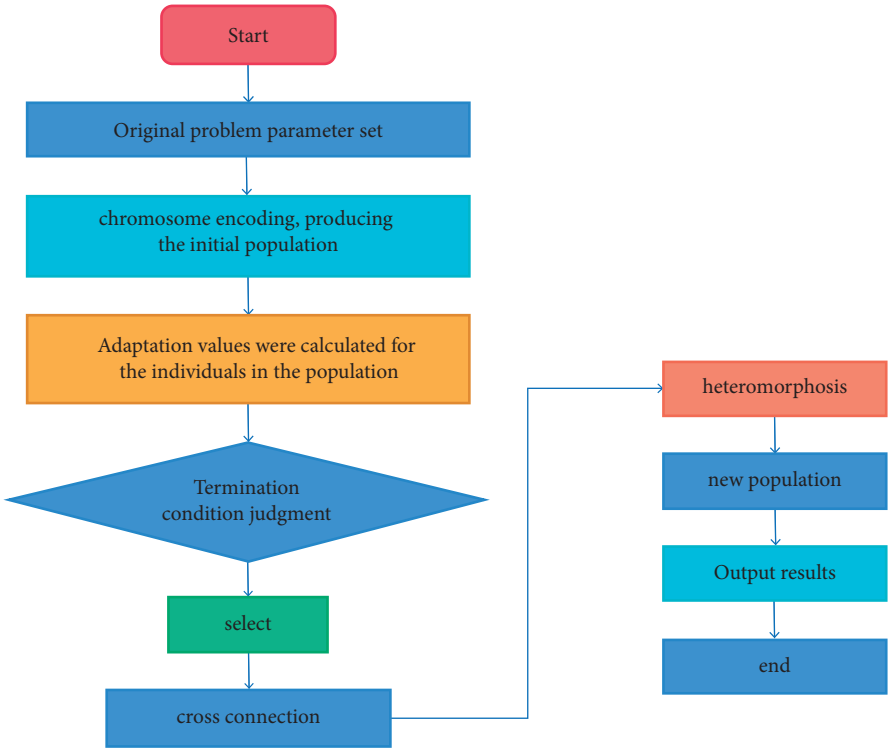

Figure 3: Genetic algorithm optimization flow chart.

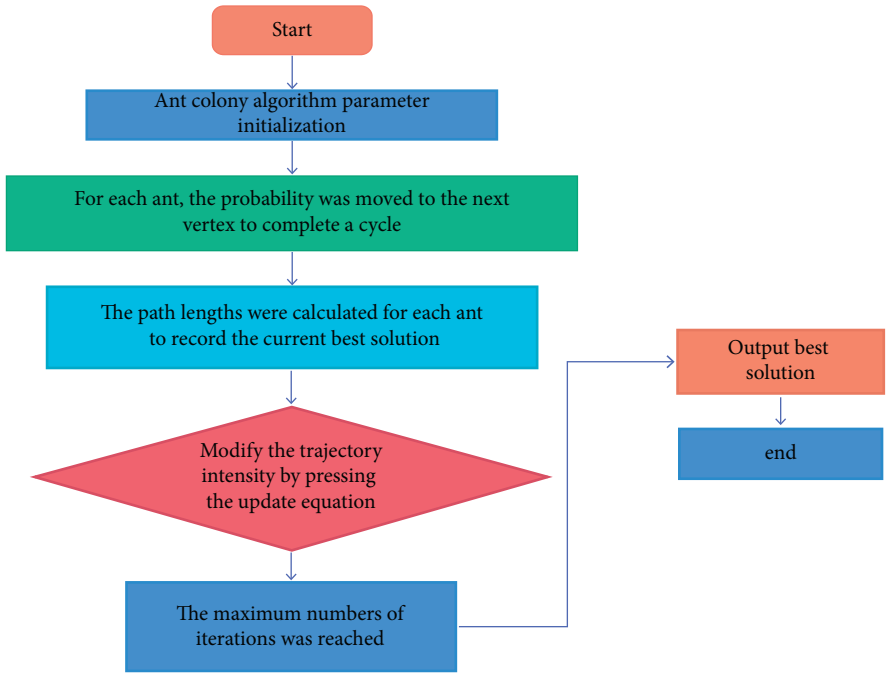

Figure 4: Flow chart of ant colony algorithm.

search is used globally, which makes the algorithm more likely to obtain the optimal solution. The flow of ant colony algorithm is shown in Figure 4.

3.3.4. Improved Particle Swarm Optimization Algorithm. The basic steps of the algorithm are as follows:

(1) The size n of the population optimized by the particle swarm optimization algorithm is selected, and the initial learning factors C1 and C2, random numbers R1 and R2, inertia weight W, search space dimension, convergence accuracy, and maximum number of iterations T are set.

(2) Initialize the speed and position of particles;

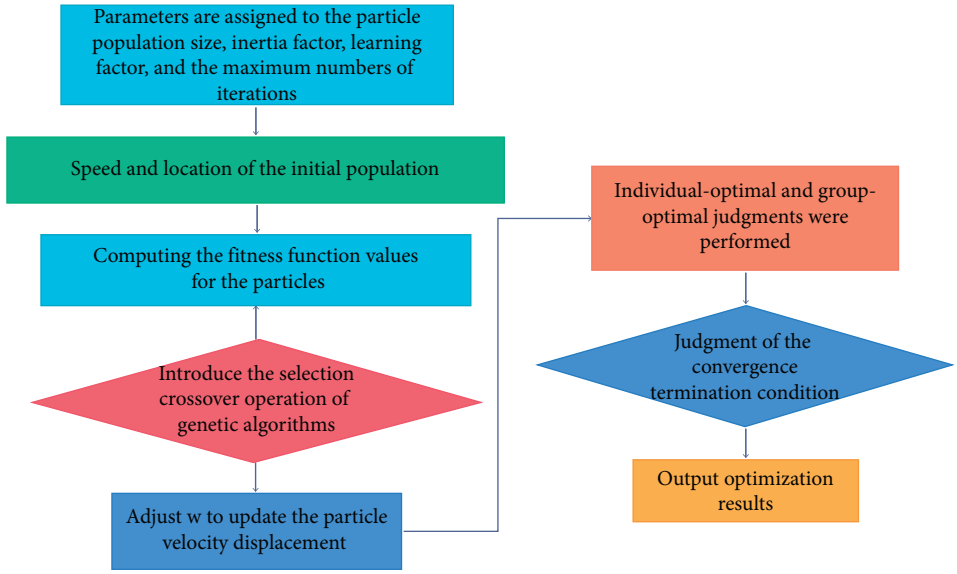

Figure 5: Flow chart of improved particle swarm optimization algorithm.

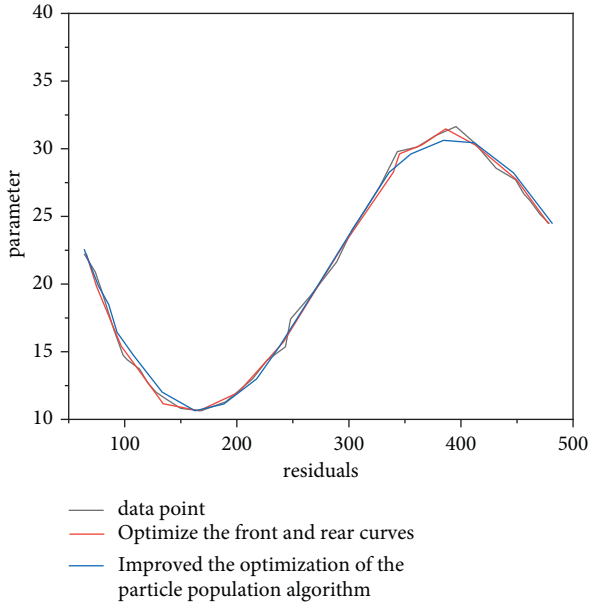

Figure 6: Curve before and after optimization and its accuracy.

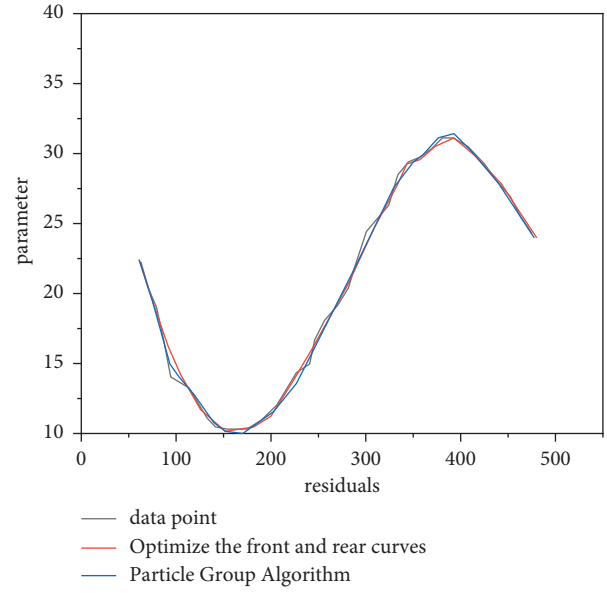

Figure 7: Optimization curve of basic particle swarm optimization algorithm and its accuracy.

(3) The fitness value of each particle is calculated and sorted, in which each particle is regarded as its individual best and stored in pbest, and the particle with the smallest fitness value in pbest is regarded as the global optimal value and stored in gbest.

(4) The selection and crossover operations in the genetic algorithm are introduced (in each iteration process, half of the particles with good fitness value are taken to directly enter the next generation, and the other half of the particles are crossed in pairs to produce new offspring. These offspring are compared with the parent generation, and then, half of the particles are selected to enter the next generation cycle).

(5) Until the termination conditions of the algorithm are met and satisfactory results are obtained, otherwise return to step (3), recalculate, and finally find the optimal solution as shown in Figure 5.

According to the operation steps of the improved particle swarm optimization algorithm, its main parameters are set as follows: population size $n = 50$, learning factor $C1 = C2 = 1.4962$, inertia weight $\mathrm{Wmax} = 0.95$, $\mathrm{wmin} = 0.5$, and the maximum number of iterations $t = 500$. The specific procedures are as follows. The optimized control points are

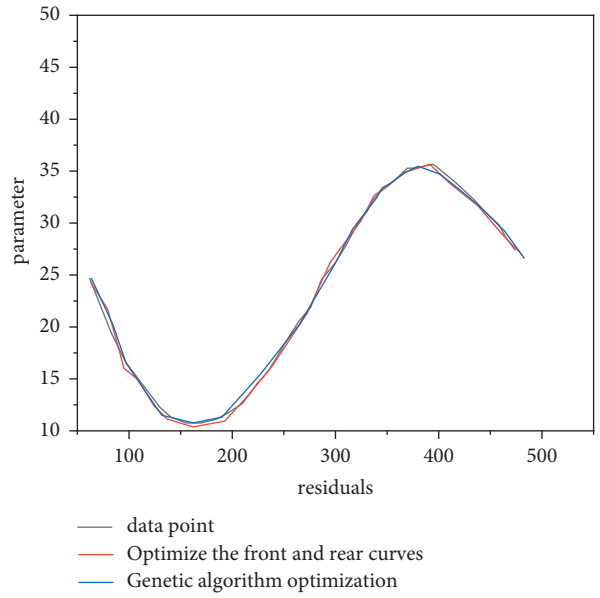

Figure 8: Optimization curve of genetic algorithm and its accuracy.

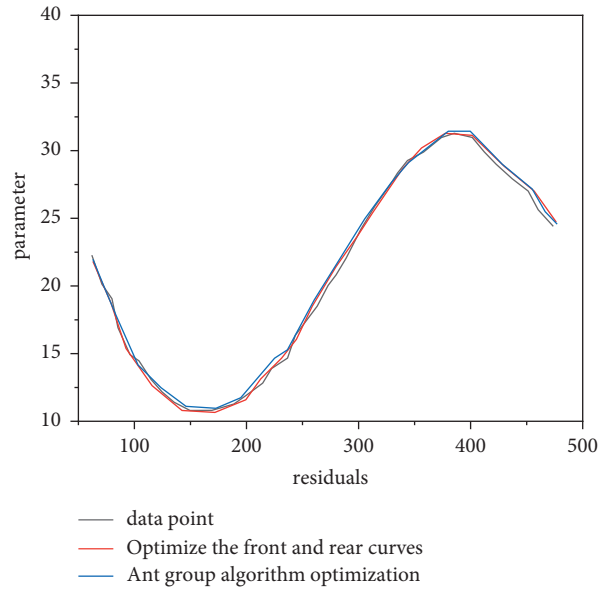

Figure 9: Optimization curve and accuracy of ant colony algorithm.

shown later. In practical operation, it tends to be stable after 250 generations. The specific calculation results are shown in Figure 6.

It can be seen from the above figure that the curve optimized by the improved particle swarm optimization algorithm is smoother, and its accuracy is higher. From the iterative process diagram, it can be seen that its operation speed is also very fast, nearly twice that of the general genetic algorithm. Therefore, it is very effective to use the minimum double energy method with physical and geometric constraints for modeling and calculation by the improved particle swarm optimization algorithm [19].

3.3.5. Comparison between the Optimization Results of Improved Particle Swarm Optimization Algorithm and Other Algorithms. The optimization effects obtained by using different algorithms are quite different. The followings are the curve effects optimized by several algorithms, as shown in Figures 7–9.

It can be seen from the above figures that the fairing effect of using the improved particle swarm optimization algorithm on the curve is much better than that of using the particle swarm optimization algorithm, genetic algorithm, and ant colony algorithm. It has high precision and fast convergence speed.

3.4. Optimization of Product Fading Surface Modeling Design

3.4.1. Block Template Matching Design of Product Fading Surface Modeling. This paper proposes a design method of product fading surface modeling based on visual expression and surface fusion. According to the method of image fusion, the coordinates of visual feature points of product fading surface modeling are $X = (x_{i0}, x_{i1}, \ldots, x_{i(n-1)}, y_{i0}, y_{i1}, \ldots, y_{i(n-1)})^T$. In the affine invariant region, the distribution state of visual features of product fading surface modeling is

$$x(n) = \sum_{k=1}^{p} a_i x(n-k) = \sum_{r=0}^{m} b_r u(n-r). \tag{13}$$

Extract the local information entropy centered on point (i, j), and analyze the dynamic characteristics of the image in the block area of the visual image of product fading surface modeling. Formulate the fusion rules according to the characteristics of local information entropy. The visual feature reconstruction model of the output fading surface modeling is obtained as follows:

$$g(x, y) = f(x, y) = \varepsilon(x, y). \tag{14}$$

Assuming that the geometric feature vector $e_1, e_2, \ldots, e_I$ of the first l visual image of product fading surface modeling, and the local information entropy represents more image detail structure, the visual reconstruction output of product fading surface modeling is obtained as follows:

$$g(t) = \sqrt{s} f(s[t-\tau]). \tag{15}$$

Among them, $f(T)$ is the local texture feature of the visual image of product fading surface modeling, $s = (c-v)/(c+v)$, which represents the scale factor of Harris corner detection. To sum up, the block template matching of product fading surface modeling is carried out, and the modeling design is carried out according to the block template matching results [20, 21].

3.4.2. Visual Optimization Control Model of Product Fading Surface Modeling. The visual optimization control model of product fading surface modeling is established, and the optimal design of product fading surface modeling is realized by combining the block fusion matching method. The

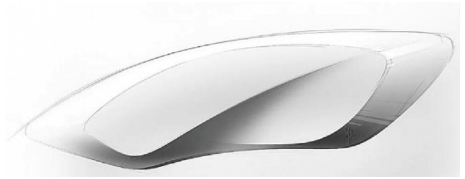

Figure 10: Initial contour modeling of fading surface of product.

Figure 11: Optimization of product fading surface modeling.

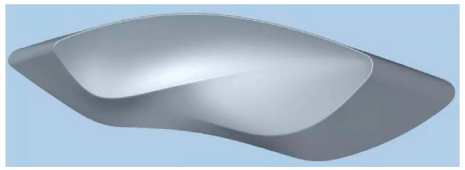

Figure 12: Modeling design of fading surface of the product.

Table 1: Performance comparison.

Method	Paper method	Genetic algorithm	Basic ant colony algorithm	Improved particle swarm optimization
Feature matching points	2543	532	1002	904
Feature resolution/%	97.45	88.55	90.32	91.231
Time cost/ms	2.45	7.34	10.23	13.23

iterative equation of visual output control of product fading surface modeling is obtained as follows:

$$W(n+1) = W(n) - \eta \frac{\partial \mathrm{E}}{\partial W} = \partial \Delta\, W(n). \tag{16}$$

After n-step training and learning, the coupling control method is adopted to obtain the dynamic characteristic process of visual reconstruction of product fading surface modeling, which is

$$w_{sij}(n_0+1) = w_{sij}(n_0) - \eta_{sij} \frac{\partial J}{\partial w_{sij}}. \tag{17}$$

The classical fusion rule is to group and fuse the pixel eigenvalues of the product fading surface modeling, extract the outline of the dark side of the visual image of the product fading surface modeling, and consider the correlation between the pixel neighborhoods to obtain a surface modeling design area with 2^I times the width of the time window. The edge windows of the product fading surface modeling design are obtained as follows:

$$I_1(n_1, n_2) = \frac{1}{4} \sum_{i1=0}^{1} \sum_{i2=0}^{1} I_{I-1}(2_{n1} + i_1, 2_{n2} + i_2). \tag{18}$$

$$J_1(n_1, n_2) = \frac{1}{4} \sum_{i1=0}^{1} \sum_{i2=0}^{1} J_{I-1}(2_{n1} + i_1, 2_{n2} + i_2). \tag{19}$$

The visual optimization control model of product fading surface modeling is established, and the optimization design of product fading surface modeling is realized by combining the block fusion matching method. To sum up, the optimization design of product fading surface modeling is realized.

4. Result Discussion

In order to test the application performance of this method in the realization of product fading surface modeling design, the simulation experiment is carried out based on rhino modeling software. The algorithm design part of image visual processing

is designed by Matlab 7. The pixel level of initial sampling of product fading surface modeling visual image is set as 1200×800, and the scale of visual feature reconstruction of product fading surface modeling visual image is set as 12, The characteristic decomposition value of regional pixel fusion is DXY = 3, the interference intensity is −10 dB, the pheromone intensity in the image is 50 dB, and the resolution of product fading surface modeling reconstruction is 2000 ∗ 2000piex. According to the above simulation parameter settings, the product fading surface modeling design is carried out to obtain the initial contour modeling of the product fading surface, as shown in Figure 10.

Taking the product fading surface in Figure 10 as the research object, the image visual imaging method is used for image fusion and filtering in the modeling design process of the product fading surface, and the output results are shown in Figure 11.

According to the analysis of Figure 11, the optimization of product fading surface modeling design can be realized by using this method. On this basis, the product fading surface modeling design output is obtained, as shown in Figure 12. According to the analysis of Figure 12, the effect of product fading surface modeling design by this method is good, and the design quality is high. Test the effect of different methods on product fading surface modeling design, and the comparison results are shown in Table 1. The analysis shows that the effect of this method on product fading surface modeling design is better.

By analyzing the results in Table 1, it can be seen that the feature resolution of product fading surface modeling design by this method is the best, with a resolution of 97.45%, short time overhead, and only 2.45 ms.

5. Conclusion

In this paper, a product fade surface modeling design method based on visual expression and surface fusion is proposed. From the perspective of computer, rhino modeling software is applied in product fade surface modeling design, the visual expression model of product fade surface modeling is constructed, and the image fusion and filtering processing in the process of product fade surface modeling design is carried out by using image visual imaging method. The edge contour features of the visual image of product fading surface modeling are extracted, the block template matching the design of product fading surface modeling is carried out by using the template block matching method, the visual optimization control model of product fading surface modeling is established, and the optimization design of product fading surface modeling is realized by combining the block fusion matching method.

Data Availability

No data were used to support this study.

Conflicts of Interest

The author declares no conflicts of interest.

References

[1] I. N. Vikhareva, G. K. Aminova, A. I. Moguchev, and A. K. Mazitova, "The effect of a zinc-containing additive on the properties of pvc compounds," *Advances in Polymer Technology*, vol. 2021, no. 3, pp. 1–14, 2021.

[2] Y. Fan, S. Wang, H. Wang, J. Xu, Q. Xiao, and Y. Wei, "Formation mechanism and chaotic reinforcement elimination of the mechanical stirring isolated mixed region," *International Journal of Chemical Reactor Engineering*, vol. 19, no. 3, pp. 239–250, 2021.

[3] D. Kong, G. He, H. Pan, Y. Weng, N. Du, and J. Sheng, "Influences and mechanisms of nano-c-s-h gel addition on fresh properties of the cement-based materials with sucrose as retarder," *Materials*, vol. 13, no. 10, pp. 2345–2349, 2020.

[4] Y. Zengyuan, Y. Cai, B. Liu, W. Weijie, and X. Chen, "Application of spherical magnetic bearing in magnetically suspended control and sensitive gyro," *Mathematical Problems in Engineering*, vol. 2020, no. 2, pp. 1–11, 2020.

[5] G. Zhang, C. Huang, J. Li, and X. Zhang, "Constrained coordinated path-following control for underactuated surface vessels with the disturbance rejection mechanism," *Ocean Engineering*, vol. 196, no. Jan.15, p. 106725, 2020.

[6] I. Nishida and K. Shirase, "Machining time reduction by tool path modification to eliminate air cutting motion for end milling operation," *International Journal of Automation Technology*, vol. 14, no. 3, pp. 459–466, 2020.

[7] K. Kikunaga, "System for visualizing surface potential distribution to eliminate electrostatic charge," *Sensors*, vol. 21, no. 13, pp. 4397–4402, 2021.

[8] D. P. Burduhos-Nergis, P. Vizureanu, A. V. Sandu, and C. Bejinariu, "Phosphate surface treatment for improving the corrosion resistance of the c45 carbon steel used in carabiners manufacturing," *Materials*, vol. 13, no. 15, pp. 3410–3415, 2020.

[9] A. Messaoudene, M. R. Mekideche, B. Bendahmane, B. Tabti, K. Medles, and L. Dascalescu, "Optimization of the active neutralization of polypropylene film using response surface methodology," *IEEE Transactions on Industry Applications*, vol. 56, no. 5, pp. 5463–5471, 2020.

[10] H. Wang, Y. Wang, Y. Zhu, F. Sun, S. Wu, and Q. Zhao, "Method to eliminate thermal disturbance errors in digital image correlation measurement based on projection speckle," *Applied Optics*, vol. 59, no. 33, pp. 10474–10478, 2020.

[11] E. D. Tetteh, Z. Qin, and B. Kwofie, "Computer-mediated communication portal implementation framework: a higher education institutional perspective," *International Journal of Emerging Technologies in Learning (iJET)*, vol. 15, no. 03, pp. 180–186, 2020.

[12] F. Ali and S. Khusro, "Content and link-structure perspective of ranking webpages: a review," *Computer Science Review*, vol. 40, no. May 2021, pp. 100397–100418, 2021.

[13] X. Wang, "Building a parallel corpus for English translation teaching based on computer-aided translation software," *Computer-Aided Design and Applications*, vol. 18, no. S4, pp. 175–185, 2021.

[14] C. Sun, "Research on investment decision-making model from the perspective of "internet of things + big data," *Future Generation Computer Systems*, vol. 107, no. Jun, pp. 286–292, 2020.

[15] B. Jacobs, "A channel-based perspective on conjugate priors," *Mathematical Structures in Computer Science*, vol. 30, no. 1, pp. 44–61, 2020.

[16] M. Nakayama, E. Hustad, and N. Sutcliffe, "Agility and system documentation in large-scale enterprise system projects: a knowledge management perspective," *Procedia Computer Science*, vol. 181, no. 1, pp. 386–393, 2021.

[17] S. I. Al-Adwan and A. s. A. h. Habahbeh, "Investigating the adoption of erp systems: a perspective from case study in Jordan," *Journal of Information Technology Research*, vol. 13, no. 1, pp. 96–117, 2020.

[18] F. Belkadi, E. Sanfilippo, A. Bernard, and L. Vidal, "A product-process model for decision-aid perspective in additive manufacturing field," *Computer-Aided Design and Applications*, vol. 17, no. 6, pp. 1278–1293, 2020.

[19] K. Wang and L. Wang, "Detect slitheen by analyzing the browsing behaviors and forcing retransmission," *Future Generation Computer Systems*, vol. 106, no. May, pp. 333–346, 2020.

[20] Z. Yan, C. Du, and L. Zhang, "Surface micro-reflector array for augmented reality display," *IEEE Photonics Journal*, vol. 12, no. 2, pp. 1–9, 2020.

[21] M. Quanjin, M. Rejab, M. Idris, N. M. Kumar, M. Abdullah, and G. R. Reddy, "Recent 3d and 4d intelligent printing technologies: a comparative review and future perspective," *Procedia Computer Science*, vol. 167, no. 9, pp. 1210–1219, 2020.